

## OBTAINING OF THIN LSM FILMS ON YSZ SUBSTRATES BY DIP COATING

D.P. Tarragó<sup>(1),\*</sup>; T.S. Bassani<sup>(1)</sup>; L. Fronza<sup>(1)</sup>; C.F. Malfatti<sup>(1)</sup>; V.C. Sousa<sup>(1)</sup>

<sup>(1)</sup> Programa de Pós-graduação em Engenharia de Minas, Metalúrgica e de Materiais (PPGE3M), Universidade Federal do Rio Grande do Sul (UFRGS)

\* Av. Bento Gonçalves, 9500, Setor IV, Prédio 74, Sala 125 – Agronomia – Porto Alegre/RS, CEP: 91501-970, Brazil

### ABSTRACT

The use of thin films in SOFC and IT-SOFC can improve their performance and lower their costs. In these devices, the cathode/electrolyte interface has direct influence in their global efficiency. The use of cheap methods, such as dip coating, calls attention for its versatility, simplicity and wide use in advanced ceramics. In this sense, two aqueous LSM dispersions were prepared to be deposited by dip coating in dense YSZ substrates. The PVP to LSM ratio added to the dispersions modified their viscosity and the substrates, after dipped, were withdrawal with different speeds. The use of constant withdrawal speeds formed more discontinuous films, although they were also discontinuous when growing withdrawal speeds were used. A thicker film was obtained using the more viscous dispersion and the higher withdrawal speeds. The dispersions' viscosity reflected in the aggregates microstructure and the LSM/YSZ diffusion interfaces for most of the samples were around 5  $\mu\text{m}$  long.

Keywords: LSM, dip coating, SOFC

### INTRODUCTION

The development of thin lanthanum strontium manganite (LSM) films using inexpensive techniques is an important step in order to apply this material in solid oxide fuel cells (SOFC) cathodes and intermediate temperature solid oxide fuel cells (IT-SOFC) composite cathodes, because many advantages outcome from the use of thin films devices, including lower costs and smaller ohmic losses, improving the cells' performance and profitability<sup>(1,2,3)</sup>. The A-site doping of lanthanum manganites perovskite structure with  $\text{Sr}^{2+}$  ions is rather chosen in low amounts, improving the

powder sinterability and enhancing the thermal stability against 8% yttria-stabilized zirconia (YSZ), which is commonly used as electrolyte<sup>(4,5)</sup>.

An intimate contact between the porous LSM film and the YSZ electrolyte must occur to increase the triple phase boundaries (TPB) active sites, where the oxygen molecule is simultaneously in contact with the cathode and the electrolyte and the reduced oxygen can be easily transported to the anode, recombining with the H<sup>+</sup> ions. Amongst with the rise of TPB sites a well-controlled microstructure, which favors the gas flow through the cathode, can improve the SOFC performance, given that the cathode performance limits the overall efficiency<sup>(6,7,8)</sup>. Since 90% of all electrochemical reactions occur at less than 10 µm from the electrode/electrolyte interface, according to numerical modeling results, there is no need for the electrodes thickness to be greater than this<sup>(9)</sup>.

The dip coating technique is widely used in the processing of advanced ceramics and is an interesting method for the study of SOFC and IT-SOFC cathode/electrolyte interfaces, once it allows the fabrication of a symmetrical cell in one step process, besides dip coating is also employed in the processing of actual fuel cell components<sup>(10,11,12,13,14)</sup>. In this work, a preliminary study was carried out using dense YSZ substrates dipped in aqueous LSM dispersions attempting to the influence of the withdrawal speed and the dispersion apparent viscosity in the final microstructure and thickness of the sintered films and to the atomic diffusion through the LSM/YSZ interface.

## **MATERIALS AND METHODS**

For the fabrication of the dense substrates a commercial grade of YSZ powder (Sigma-Aldrich) was ball milled in ethanol with the addition of 3% of polivinylbutyral (PVB) to act as binder. The dry powder was uniaxially compacted at 175 MPa, after an 85 MPa pre-load, in 12 mm diameter discs. The green YSZ bodies were sintered at 1450°C for 90 min and a politetrafluoroethylene (PTFE) tape was used to mask the samples sides allowing the deposition only in the disc faces. Simple measurements of mass and volume of the sintered bodies were used to determine the substrates densification and a CETR PRO500 3D profilometer was used to analyze the surface roughness within an area of 62500 µm<sup>2</sup>. The roughness values were expressed as arithmetic average of the absolute values of deviation from the base line (Ra), the roughness quadratic average (Rms) and the peak to peak maximum distance (Ry).

The LSM dispersions were prepared using a combustion obtained  $\text{La}_{0.9}\text{Sr}_{0.1}\text{MnO}_3$  powder, with specific surface area of  $45.0 \text{ m}^2/\text{g}$  and two dispersions were prepared according to the recipe in Table 1. The powder was dispersed in distilled water in an ultrasonic bath and polyvinylpyrrolidone (PVP) was dissolved in the dispersions to modify their viscosity. The dispersions' apparent viscosity was determined by a Brookfield DV-II apparatus with a CP-40 plate rotating at 100 rpm and at the temperature of  $25^\circ\text{C}$ .

Table 1: PVP and water ratios used in the preparation of the dispersions.

Dispersion	PVP to LSM mass ratio	H <sub>2</sub> O to LSM ml to g ratio
D1	0.5 : 1	6.5 : 1
D2	1 : 1	6.5 : 1

A total of nine YSZ substrates were used, being six dipped in the dispersion D1 and the other three dipped in the dispersion D2. Table 2 illustrates the amount of baths and the withdrawal speeds used for each substrate and all films were sintered at  $1200^\circ\text{C}$  for 60 minutes, remaining 90 minutes at  $750^\circ\text{C}$  during the heating and plus 90 minutes at the same temperature during the cooling.

Table 2: Dip coating parameters used in each substrate and samples names.

Sample	Dispersion used	Withdrawal speed (mm/min)
D1-5	D1	5 / 5 / 5
D1-10	D1	10 / 10 / 10
D1-25	D1	25 / 25 / 25
D2-5	D2	5 / 5 / 5
D2-10	D2	10 / 10 / 10
D2-25	D2	25 / 25 / 25
D1-A	D1	5 / 10 / 25 / 50
D1-B	D1	5 / 5 / 10 / 10 / 25 / 25 / 50 / 50
D1-C	D1	10 / 25 / 50 / 100

After sintering the films were observed in a scanning electron microscopy (SEM) and most of them were analyzed by energy dispersion spectrometer (EDS)

probe using a point by point quantitative analysis in order to evaluate the LSM/YSZ interface.

## RESULTS AND DISCUSSION

The YSZ substrates reached a densification of 97.6% ( $\pm 1.6\%$ ). The 3D surface profile of the YSZ substrates generated in the profilometer is shown in Figure 1 and Table 3 contains the results of the roughness parameters. As seen, the substrates were as rough as 0.25  $\mu\text{m}$ .

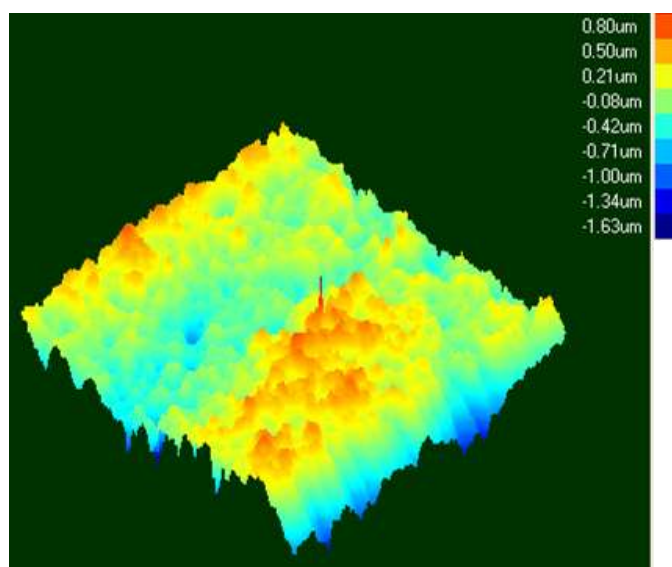


Figure 1: Surface 3D profile of an YSZ substrate.

Table 3: Profilometer roughness results.

Sample	Ra ( $\mu\text{m}$ )	Rms ( $\mu\text{m}$ )	Ry ( $\mu\text{m}$ )
YSZ substrate	0.248	0.313	3.056

The apparent viscosity of the prepared dispersions are in Table 4. When the amount of PVP in the dispersion doubled, as in the dispersion D1 to dispersion D2, a significant increase in the apparent viscosity could be verified.

Table 4: Dispersions apparent viscosity.

Sample	Apparent viscosity (mPa.s)
D1	20.1
D2	88.4

After sintering the films a dark layer was formed on both faces of the substrates, which had its side preserved by the PTFE mask. Figure 2 shows two YSZ substrates, in the left: before dipping; and in the right after dipping and sintering the LSM film.

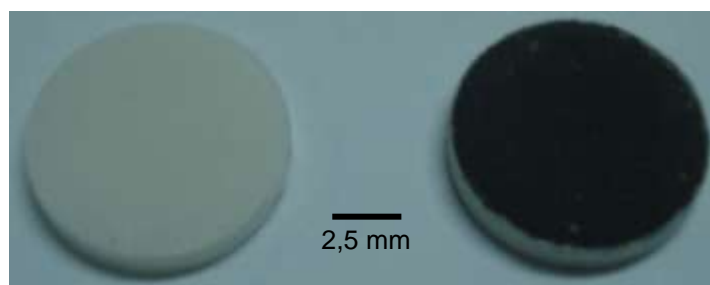


Figure 2: YSZ substrates before and after the dip coating.

The SEM micrographs of the films obtained with both dispersions and with baths with same withdrawal speed are shown in Figure 3, amongst with those obtained with growing withdrawal speed. From the samples with same withdrawal speed, it is observed that all films formed from the low viscosity dispersion (D1) were highly discontinuous. The use of high withdrawal speed and the more viscous dispersion in sample D2-25 promoted the obtaining a thin film with some continuity though it also seemed to be very fragile.

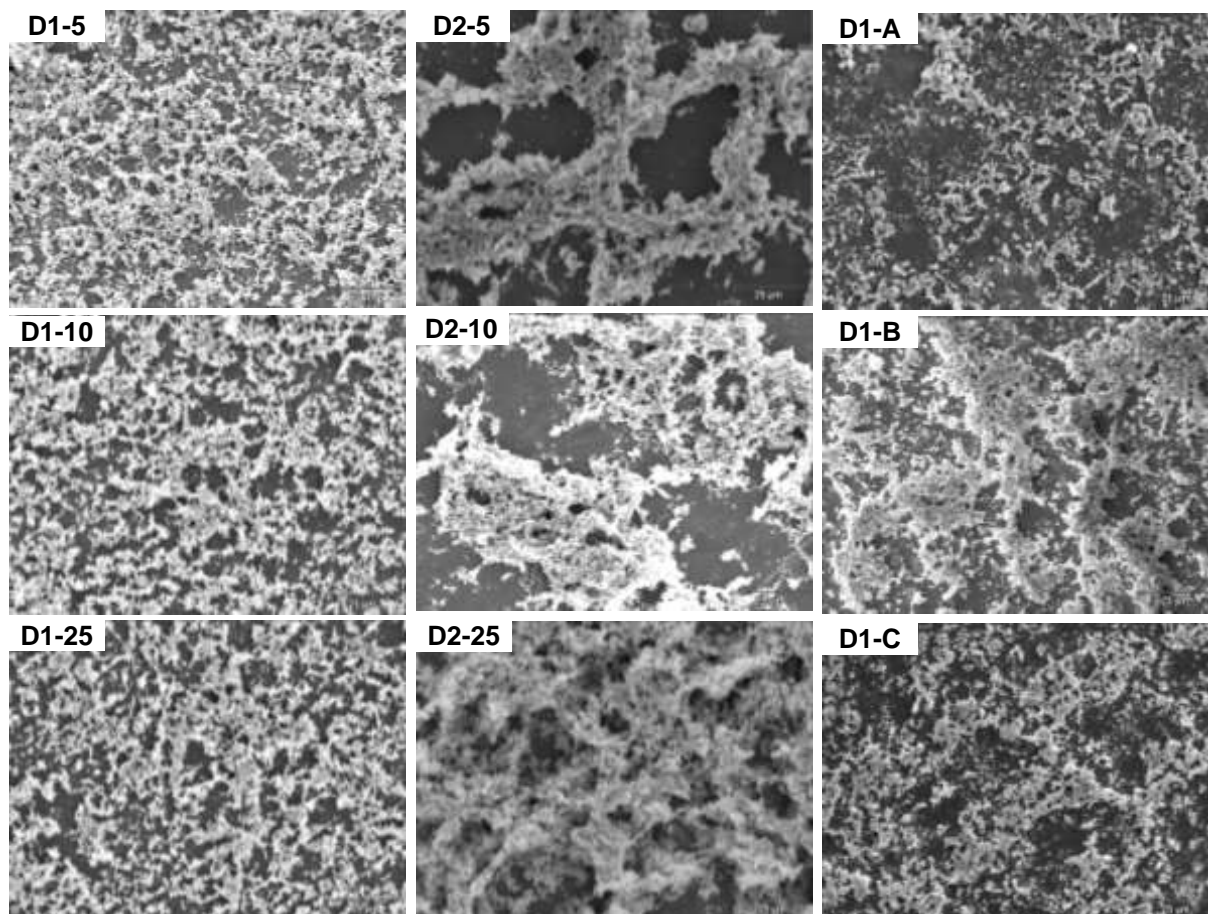


Figure 3: SEM micrographs from the top of the LSM films.

Comparing the films obtained with same withdrawal speeds it is possible to distinguish the influence of the dispersion viscosity, where higher apparent viscosity resulted in larger aggregates while lower apparent viscosity tend to spread wider the powder forming small aggregates.

When the withdrawal speed varied in the same sample the films formed seemed to be more continuous over the substrate and they also appeared very dense in some areas. The procedure used in these samples could have put the LSM particles in a closer contact favoring the formation of continuous films and leading to a higher densification spots.

In the EDS results of samples dipped with same withdrawal speeds, in Figure 4, it can be seen that the LSM/YSZ diffusion interface is a few micrometers long for sample D1-25 and in the sample D2-25 its size oddly raises to around 35  $\mu\text{m}$ .

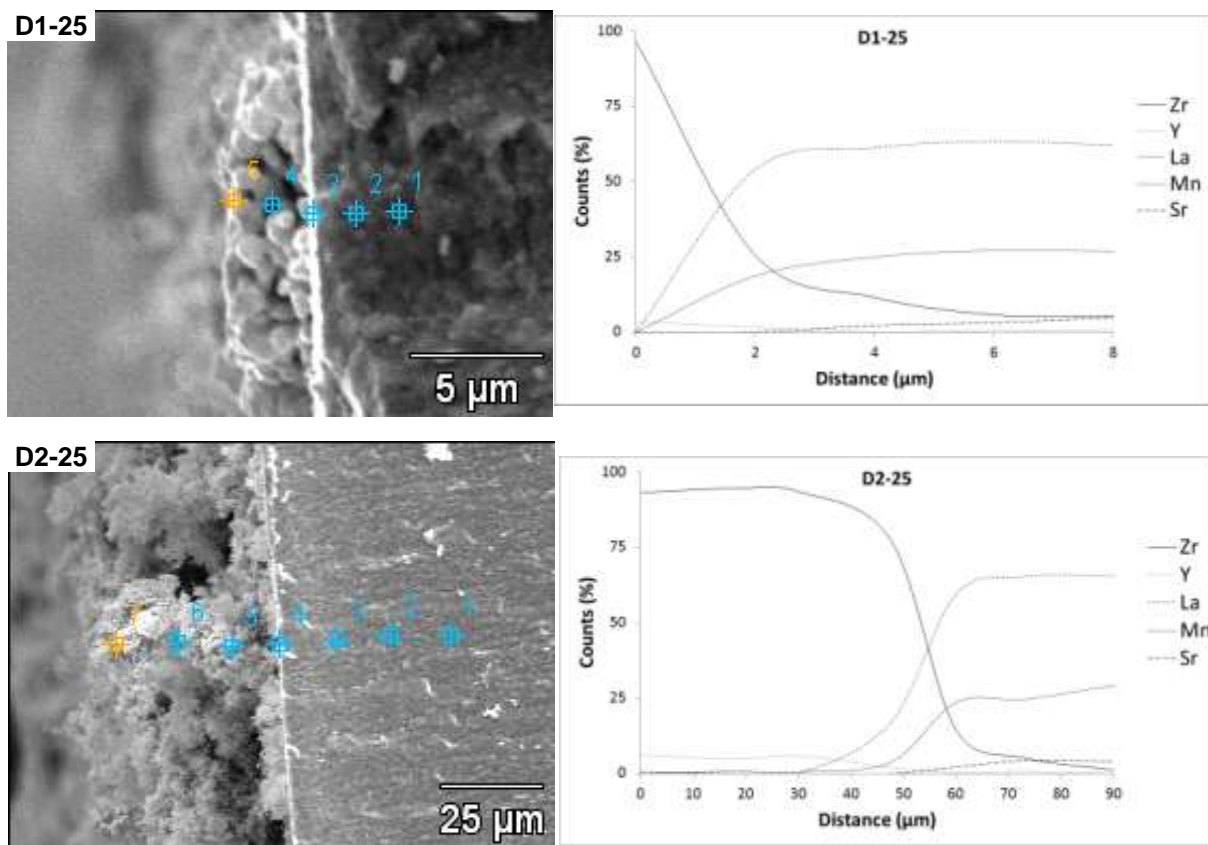


Figure 4: Cross section SEM micrographs and EDS results from samples with constant withdrawal speeds.

These samples differ only by the amount of PVP in the dispersion and the film thickness, which was around 5 µm for sample D1-25 and almost 50 µm for sample D2-25, thus it is assumed that one of these parameters could have contributed for this interface size increment.

In Figure 5 are shown the SEM micrograph together with the EDS results for the samples dipped in dispersion D1 and withdrawal with growing speeds.

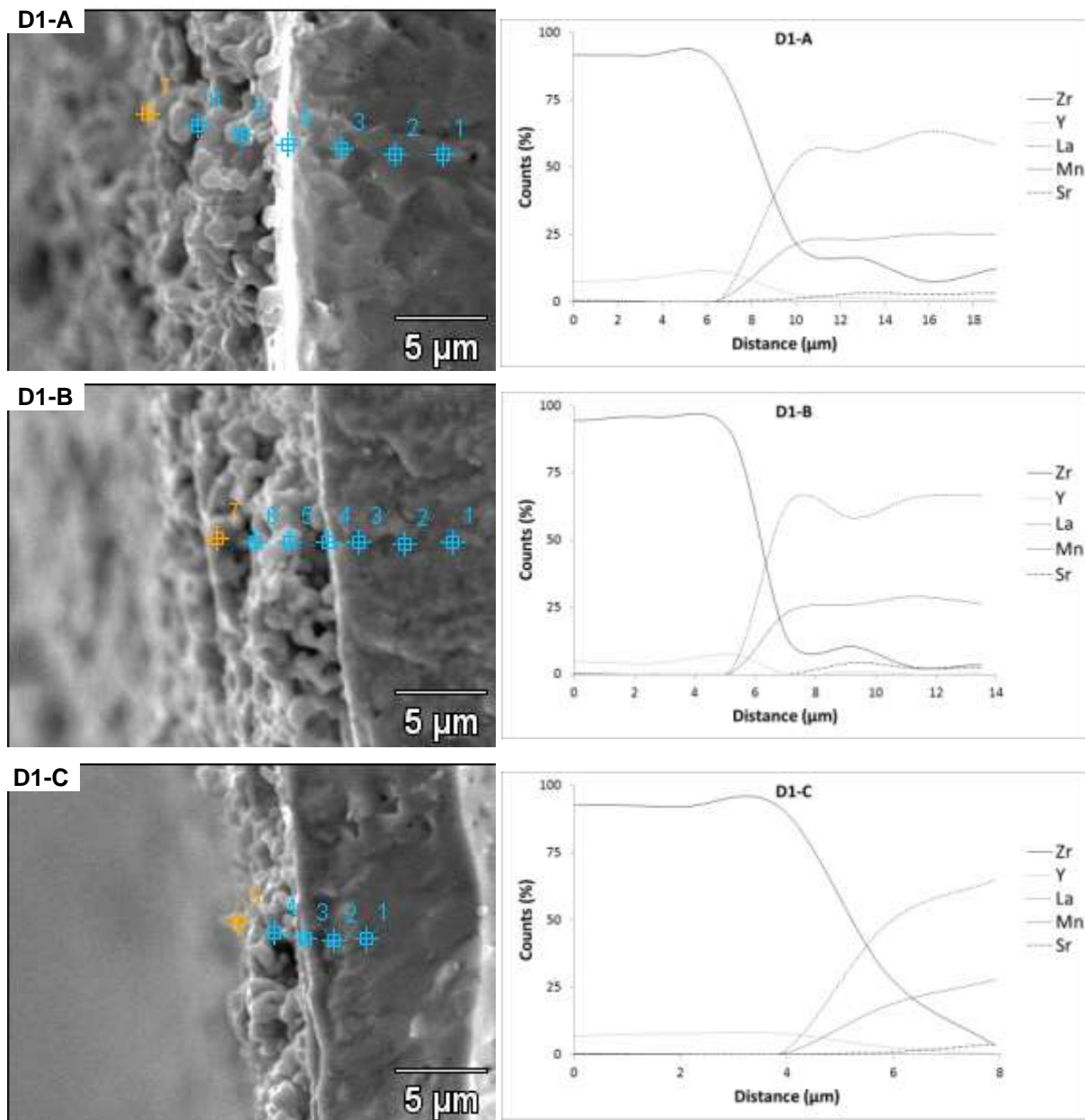


Figure 5: Cross section SEM micrographs and EDS results from samples with growing withdrawal speeds.

The films thickness did not seemed to be greatly influenced by the different withdrawal speeds and this could be related to powder removal during the submerged time between the consecutive baths. Also, the LSM/YSZ interface did not suffer the influence of the withdrawal speeds and was very close in size to that observed in sample D1-25.

## CONCLUSIONS

The thin LSM films dip coated in the YSZ substrates formed a diffusion interface where atoms from LSM diffuse into a limited distance of the electrolyte and the YSZ atoms as well diffuse into the cathode. This interface, measured by EDS point by point scan, was around 5  $\mu\text{m}$  for all samples except for the D2-25. In spite of this contact interface formed, most of the films were discontinuous. Those fabricated with growing withdrawal speeds also did not form continuous films, although they appeared quite denser in the micrographs.

PVP did manage the dispersions' viscosity and, even though the films were discontinuous, it reflected in the films microstructure. The less viscous dispersion D1 tends to spread the aggregates in the substrate surface which were, then, smaller than those formed with the more viscous dispersion D2.

## ACKNOWLEDGEMENTS

The authors would like to thank to the CNPq for the financial support and to Jomon Advanced Ceramics for the donated material.

## REFERENCES

- (1) SAHU, A.K.; GHOSH, A.; SURI, A.K. Characterization of lanthanum strontium manganite (LSM) and development of yttria stabilized zirconia (YSZ) coating. *Ceram. Int.*, v.35, p.2493, 2009.
- (2) HONGYAN, S.; WENHUI, M.A.; JIE, Y.; XIUHUA, C.; HANGSHENG, L. Preparation and characterization of  $\text{La}_{0,8}\text{Sr}_{0,04}\text{Ca}_{0,16}\text{Co}_{0,6}\text{Fe}_{0,4}\text{O}_{3-\delta}$ - $\text{La}_{0,9}\text{Sr}_{0,1}\text{Ga}_{0,8}\text{Mg}_{0,2}\text{O}_3$  composite cathode thin film for SOFC by slurry spin coating. *J. Rare Earths*, v.28, p.917, 2010.
- (3) EG&G TECHNICAL SERVICES; SCIENCE AND APPLICATIONS INTERNATIONAL CORPORATION. Fuel Cell Handbook. Morgantown: U.S. Department of Energy, ed.6, 2002.
- (4) YOKOKAWA, H.; SAKAI, N.; KAWADA, T.; DOKYIA, M. Thermodynamic stabilities of perovskite oxides for electrodes and other electrochemical materials. *Solid State Ionics*, v.52, p.43, 1992.
- (5) MEIXNER, D.L.; CUTLER, R.A. Sintering and mechanical characteristics of lanthanum strontium manganite. *Solid State Ionics*, v.146, p.273, 2002.
- (6) FLORIO, D.Z.; FONSECA, F.C.; MUCCILLO, E.N.S.; MUCCILLO, R. Materiais cerâmicos para células a combustível. *Cerâm.*, v.50, p.275, 2004.
- (7) HAANAPPEL, V.A.C.; MERTENS, J.; RUTENBECK, D.; TROPARTZ, C.; HERZHOF, W.; SEBOLD, D.; TIETZ, F. Optimization of processing and

- 
- microstructural parameters of LSM cathodes to improve the electrochemical performance of anode-supported SOFCs.  
J. Power Sources, v.141, p.216, 2005.
- (8) STEELE, B.C.H. Behaviour of porous cathodes on high temperature fuel cells.  
Solid State Ionics, v.94, p.239, 1997.
- (9) ANDERSSON, M.; YUAN, J.; SUNDÉN, B. SOFC modeling considering electrochemical reactions at the active three phase boundaries.  
Int. J. Heat. Mass. Trans., in press, 2011.
- (10) JOSE, R.; JOHN, A.M.; JAMES, J.; NAIR, K.V.O.; KURIAN, K.V.; KOSHY, J. Superconducting Bi(2223) films ( $T_C(0)=110$  K) by dip-coating on  $Ba_2LaZrO_{5.5}$ : a newly developed perovskite ceramic substrate.  
Mater. Letters, v.42, p.112, 1999.
- (11) GUNES, M.; GENCER, H.; KOLAT, V.S.; VURAL,S.; MUTLU, H.I.; SECKIN, T.; ATALAY, S. Microstructure and magnetoresistance of a  $La_{0.67}Ca_{0.33}MnO_3$  film produced using dip-coating method.  
Mater. Sci. Eng. B, v.136, p.41, 2007.
- (12) GAUDON, M.; LABERTY-ROBERT, C.; ANSART, F.; STEVENS, P.; ROUSSET, A. Preparation and characterization of  $La_{1-x}Sr_xMnO_{3+\delta}$  ( $0 \leq x \leq 0,6$ ) powder by sol-gel process.  
Solid State Sci., v.4, p.125, 2002.
- (13) ARENDT, E.; MAIONE, A.; KLISINSKA, A.; SANZ, O.; MONTES, M.; SUAREZ, S.; BLANCO, J.; RUIZ, P. Structuration of  $LaMnO_3$  perovskite catalysts on ceramic and metallic monoliths: Physico-chemical characterization and catalytic activity in methane combustion.  
App. Cat. A: General, v.339, p.1, 2008.
- (14) BAI, Y.; LIU, J.; GAO, H.; JIN, C. Dip coating technique in fabrication of cone-shaped anode-supported solid oxide fuel cell.  
J. Alloys Comp., v.480, p.554, 2009.